Optimal functional levels of activation-induced deaminase specifically require the Hsp40 DnaJa1

Alexandre Orthwein[1,2], Astrid Zahn[1], Stephen P Methot[1,6], David Godin[1], Silvestro G Conticello[3], Kazutoyo Terada[4] and Javier M Di Noia[1,2,5,6,*]

[1]Laboratory of Mechanisms of Genetic Diversity, Institut de Recherches Cliniques de Montréal, Montréal, Québec, Canada, [2]Department of Microbiology and Immunology, Université de Montréal, Québec, Canada, [3]Istituto Toscano Tumori, Firenze, Toscana, Italy, [4]Department of Molecular Genetics, Kumamoto University, Kumamoto, Japan, [5]Department of Medicine, Faculty of Medicine, Université de Montréal, Montréal, Québec, Canada and [6]Department of Medicine, Division of Experimental Medicine, McGill University, Montréal, Québec, Canada

The enzyme activation-induced deaminase (AID) deaminates deoxycytidine at the immunoglobulin genes, thereby initiating antibody affinity maturation and isotype class switching during immune responses. In contrast, off-target DNA damage caused by AID is oncogenic. Central to balancing immunity and cancer is AID regulation, including the mechanisms determining AID protein levels. We describe a specific functional interaction between AID and the Hsp40 DnaJa1, which provides insight into the function of both proteins. Although both major cytoplasmic type I Hsp40s, DnaJa1 and DnaJa2, are induced upon B-cell activation and interact with AID *in vitro*, only DnaJa1 overexpression increases AID levels and biological activity in cell lines. Conversely, DnaJa1, but not DnaJa2, depletion reduces AID levels, stability and isotype switching. *In vivo*, DnaJa1-deficient mice display compromised response to immunization, AID protein and isotype switching levels being reduced by half. Moreover, DnaJa1 farnesylation is required to maintain, and farnesyltransferase inhibition reduces, AID protein levels in B cells. Thus, DnaJa1 is a limiting factor that plays a nonredundant role in the functional stabilization of AID.

Introduction

Naive B lymphocytes display the prediversified primary repertoire of antibodies. Antibody responses are initiated when a few of them recognize their cognate antigen and proliferate. To be effective, the antibodies produced by the selected B-cell clones still need to undergo affinity maturation to better recognize the antigen; as well as isotype switching to change the default IgM isotype for IgG, IgE or IgA. Antibody affinity maturation and isotype switching absolutely depend on activation-induced deaminase (AID) (Muramatsu *et al*, 2000; Revy *et al*, 2000).

AID deaminates deoxycytidine to deoxyuridine at defined regions of the immunoglobulin (Ig) genes, which initiates somatic hypermutation or gene conversion, the molecular pathways underpinning antibody affinity maturation, as well as class switch recombination (CSR) (Di Noia and Neuberger, 2007; Peled *et al*, 2008; Stavnezer *et al*, 2008). AID deficiency compromises the antibody response resulting in a Hyper-IgM immunodeficiency syndrome (Revy *et al*, 2000). On the other hand, AID contributes to antibody-mediated autoimmune diseases (Zaheen and Martin, 2011) as well as to cancer (Okazaki *et al*, 2003; Pasqualucci *et al*, 2008). The latter ensues from AID mutating tumour suppressor and (proto)-oncogenes as well as from initiating chromosomal translocations as byproducts of CSR (Pasqualucci *et al*, 2001; Ramiro *et al*, 2004; Liu *et al*, 2008; Robbiani *et al*, 2008; Yamane *et al*, 2011). A number of regulatory pathways enforcing an appropriate AID expression pattern, optimal AID mRNA and protein levels as well as modulating its access to the nucleus, favour AID physiological functions over its pathological effects (reviewed in Stavnezer, 2011; Storck *et al*, 2011).

AID post-translational regulation is important for two reasons. First, because upwards and downwards variations in AID levels impact the frequency of both antibody diversification and pathological byproducts (Sernández *et al*, 2008; Teng *et al*, 2008; Robbiani *et al*, 2009; Orthwein *et al*, 2010). Second, because physiological and pathological expression of AID outside germinal centre B cells is well documented (Morgan *et al*, 2004; Pasqualucci *et al*, 2004; Matsumoto *et al*, 2007; Macduff *et al*, 2009; Pauklin *et al*, 2009; Kuraoka *et al*, 2011). Prominent among AID regulation are subcellular localization and protein stability, which are linked mechanisms that limit AID access to the genome. Indeed, AID is a nucleo-cytoplasmic shuttling protein but most of AID is in the cytoplasm in steady state because nuclear export plus cytoplasmic retention outcompete nuclear import (Brar *et al*, 2004; Ito *et al*, 2004; McBride *et al*, 2004; Patenaude *et al*, 2009; Patenaude and Di Noia, 2010). In turn, cytoplasmic AID is more stable than nuclear AID (Aoufouchi *et al*, 2008; Orthwein *et al*, 2010). We have shown that AID is stabilized in the cytoplasm by the chaperone Hsp90, which helps explaining the differences in AID stability depending on its localization (Orthwein *et al*, 2010). We now describe a key role for the Hsp40 DnaJa1 in determining AID protein levels and stability.

The prototypical Hsp40 is *Escherichia coli* DnaJ, a cochaperone of the bacterial Hsp70 DnaK (Langer *et al*, 1992). DnaJ is but one member of a large protein family characterized by the J-domain, which stimulates the ATPase activity of

*Corresponding author. Laboratory of Mechanisms of Genetic Diversity, Institut de Recherches Cliniques de Montreal (IRCM), 110 Avenue des Pins Ouest, Montreal, Quebec, Canada H2W 1R7.
Tel.: +1 514 987 5642; Fax: +1 514 987 5528;
E-mail: javier.di.noia@ircm.qc.ca

Hsp70 as part of a chaperoning cycle that allows folding, conformational changes, degradation and transport across membranes (Walsh *et al*, 2004; Qiu *et al*, 2006; Kampinga and Craig, 2010). The human genome encodes for 41 J-domain proteins, which can be divided into three groups (Qiu *et al*, 2006; Kampinga and Craig, 2010). Type I J-proteins or DjAs (DnaJa1–4) are orthologues of *E. coli* DnaJ and yeast Ydj1. DjAs have an N-terminal J-domain separated by a Gly/Phe-rich linker from the C-terminal substrate-binding region. This region contains three distinct structural domains revealed by the Ydj1 crystal structures (Li *et al*, 2003; Wu *et al*, 2005) (Supplementary Figure S1): CTDI, has a hydrophobic pocket that binds certain peptides found in a subset of Ydj1 substrates; CTDII, is made of two Zn-fingers; and CTDIII, which contains most residues involved in DjA dimerization. Additionally, like YdJ1, cytoplasmic DjAs have a short C-terminal extension ending in a farnesylated motive (Kanazawa *et al*, 1997). Type II J-proteins or DjBs (13 members in humans) are orthologues of yeast Sis1 and have CTDI and CTDIII structurally homologous to DjA's (Sha *et al*, 2000) but lack Zn-fingers. Type III J-proteins are very heterogeneous in structure, size and function sharing only the J-domain. Only DjAs and some DjBs behave as Hsp70 cochaperones similarly to DnaJ, Ydj1 or Sis1 (Qiu *et al*, 2006; Kampinga and Craig, 2010). Some DjAs additionally work in the Hsp90-mediated stabilization pathway (Caplan *et al*, 1995; Kimura *et al*, 1995; Hernández *et al*, 2002).

The expansion and divergence of J-protein paralogs during evolution contrast with the conservation of many orthologues across vertebrate species (f.i. DnaJa1 is >95% identical between most vertebrates). This is likely to reflect functional specialization and presumably some specific subset of substrates *in vivo*, the mechanistic details of which as well as the identity of the substrates are largely unknown (Kampinga and Craig, 2010). *In-vitro* folding experiments have shown some redundancy but also clear functional differences between the major mammalian cytosolic Hsp40s (DnaJa1, DnaJa2, Dnaja4, DnaJb1) (Terada and Mori, 2000; Bhangoo *et al*, 2007; Tzankov *et al*, 2008; Walker *et al*, 2010). The different phenotypes of mice deficient for DnaJa1 (Terada *et al*, 2005) and DnaJb1 (Uchiyama *et al*, 2006) support this view but have not provided yet the identity of any substrates that would depend on one particular Hsp40. Here, we identify DnaJa1 as a specific limiting factor in determining AID protein levels and biological activity during the immune response in mice.

Results

AID interacts with a subset of Hsp40 cochaperones and with Hsc70

Several results pointed to the interaction between AID and type I Hsp40/DjAs. A yeast two-hybrid screening using AID as bait (described in Conticello *et al*, 2008) yielded DnaJa2 (Figure 1A). Mass spectrometry then identified DnaJa1 among the proteins copurifying with AID–Flag/HA through two consecutive immunopurifications using agarose-conjugated antibodies (Orthwein *et al*, 2010), which we confirmed here by coimmunoprecipitation (coIP) (Figure 1B). Finally, DnaJa1, a2 and a3 were pulled down with AID–GFP using anti-GFP-coated magnetic beads from extracts of stably trans-

fected Ramos B cells (Table I). We verified the DnaJa1–AID interaction by coIP (Figure 1C). CoIP also confirmed the preferential association of AID with cytoplasmic DjAs compared with DnaJb1 and DnaJb11, two of the DjB members most similar to DnaJa1 (Figure 1D and E). We focused on DnaJa1 and DnaJa2, which are highly induced upon B-cell activation, excluding DnaJa4, which was undetectable (Figure 1F) and DnaJa3 because it is mitochondrial (Qiu *et al*, 2006). DjAs have Zn-fingers and *E. coli* J-proteins non-specifically bind to DNA (Gur *et al*, 2005) but nuclease treatment confirmed that AID interaction with DjAs was not mediated by nucleic acids (Figure 1G).

We previously showed that AID interacts with Hsp90 while the AID paralogs APOBECs do not despite being up to 60% similar to AID (Orthwein *et al*, 2010). Also here, AID but not APOBEC1, 2 or 3G, interacted with DnaJa1 and DnaJa2 by coIP (Figure 2A and B). The major cytosolic Hsp70 isoform, Hsc70 (encoded by *HSPA8*) was identified in our three pull-down experiments (Table I). Again, Hsc70 coIP with AID but not with any of the APOBECs from transfected cells (Figure 2C). Interestingly, the binding of DnaJa1 or DnaJa2 to AID was not equivalent. We used AID–APOBEC2 chimeras, in which 30–50 amino acids long AID regions were replaced by the homologous APOBEC2 residues (Figure 2D) (Conticello *et al*, 2008), to probe the interaction between AID and DjAs. Most chimeras partially or completely lost interaction with DnaJa1 while they all interacted with DnaJa2 just as well as AID (Figure 2E and F). We can conclude that there is a specific association of AID to DjAs and the Hsp40–Hsp70 chaperoning machinery, which is not detected for the APOBEC enzymes.

DnaJa1 determines the protein levels and activity of AID in B-cell lines

The ability of both DnaJa1 and DnaJa2 to bind to over-expressed AID may not be surprising since they share ~70% similarity (Supplementary Figure S1). Notwithstanding this, several reports suggest that they are not completely redundant in their functions (Terada *et al*, 2005; Bhangoo *et al*, 2007; Tzankov *et al*, 2008). We thus tested whether DnaJa1 and/or DnaJa2 were functionally relevant for AID biology, first through overexpression. We used the mouse B-cell line CH12F3 in which stimulation with anti-CD40, TGF-β1 and IL-4 induces AID and isotype switching to IgA (Nakamura *et al*, 1996; Muramatsu *et al*, 1999). Retroviral delivery led to ~2-fold overexpression of DnaJa1 or DnaJa2 in CH12F3 cells (Figure 3A and B). Only DnaJa1 overexpression was associated with higher AID protein levels (~1.6-fold) and a significant increase in CSR (Figure 3B and C). We obtained similar results in the chicken B-cell lymphoma line DT40, which constitutively expresses AID and undergoes Ig gene conversion (Arakawa *et al*, 2002). Overexpression of DnaJa1, but not of DnaJa2, correlated with increased levels of endogenous AID (Figure 3D and E). This was accompanied by a similar increase in the rate of Ig gene conversion as measured by a surface IgM-gain fluctuation assay (Figure 3F). In this assay, a proportion of AID-dependent gene conversions in the DT40 CL18 line reverses a frameshift in the IgVλ, thus rescuing IgM expression (Arakawa *et al*, 2002). The median proportion of IgM$^+$ cells arising during clonal expansion of multiple populations is proportional to the Ig gene conversion activity. In contrast, overexpression of Hsc70
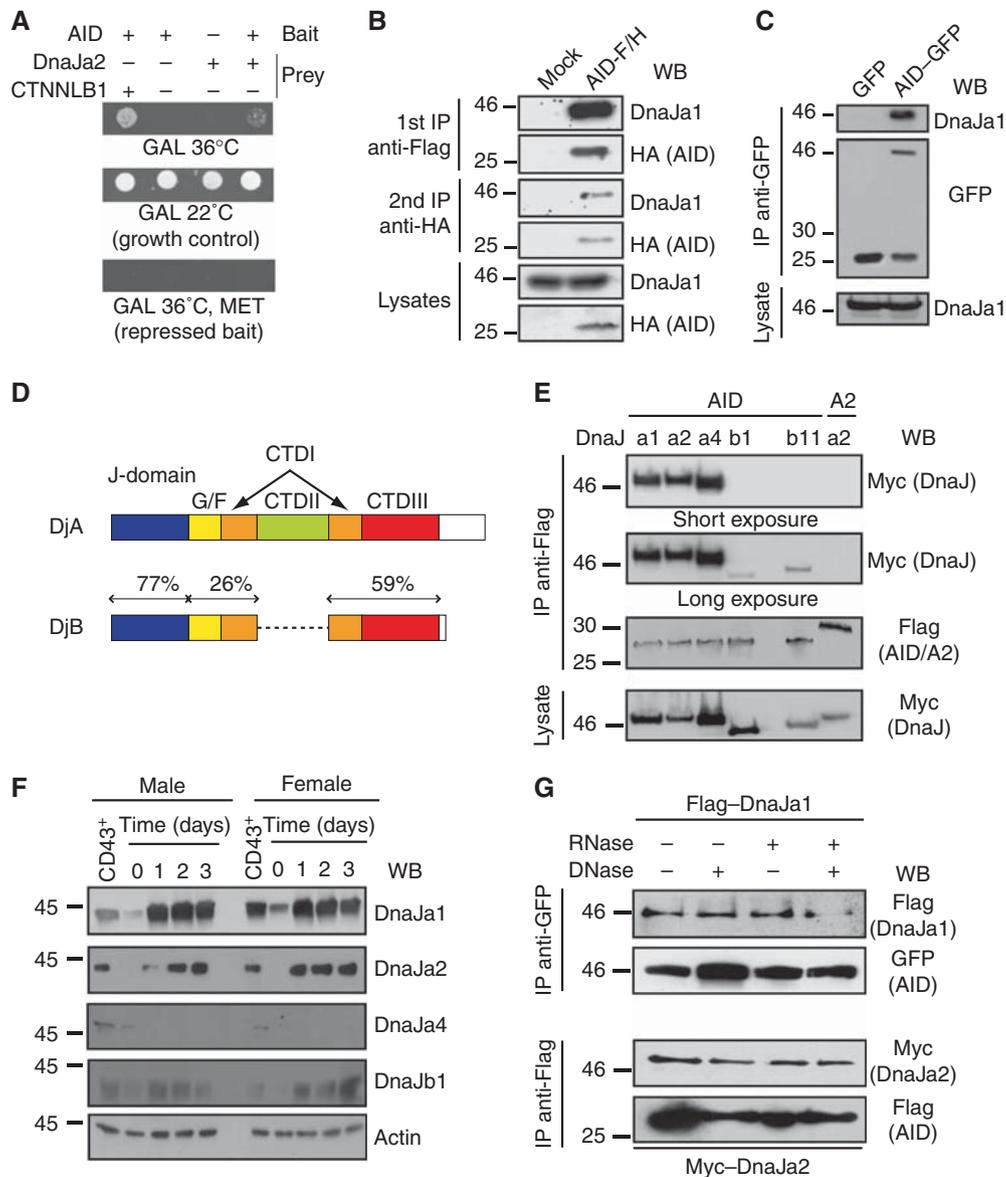
Figure 1 AID interacts with type I J-proteins. (**A**) Yeast two-hybrid assay showing the interaction of AID with DnaJa2 (truncated clone starting at codon 198). The AID-interacting protein CTNNLB1, isolated in the same screening from a human spleen library (Conticello *et al*, 2008), was used as positive control. GAL, galactose; GLU, glucose; MET, methionine. (**B**) AID–Flag/HA was sequentially immunoprecipitated using anti-Flag and then anti-HA from extracts of stably expressing Ramos cells and analysed by western blot after each step to detect endogenous DnaJa1. One of the two independent experiments is shown. (**C**) GFP or AID–GFP were immunoprecipitated from extracts of stably expressing Ramos cells and analysed as in (**B**). (**D**) Schematic structure of type I (DjA) and type II (DjB) J-proteins. Similarity values (%) for each structural domain, calculated from the alignment between DnaJa1 and DnaJb1, are indicated. (**E**) Lysates from HEK293T cells cotransfected with Flag-tagged AID or APOBEC2 (A2) and Myc-tagged versions of the indicated DnaJ proteins were immunoprecipitated with anti-Flag and analysed by western blot. One of the two independent experiments is shown. (**F**) Expression of selected DnaJ proteins in total cell lysates of mouse naive primary splenic B cells purified by CD43 depletion (>97% CD43⁻ B220+) either resting (0) or after 1–3 days stimulation with IL-4 and LPS, analysed by western blot using antibodies against DnaJa1, DnaJa2, DnaJa4, DnaJb1 and actin. The CD43-enriched fraction (a heterogeneous mixture including T, B and other leukocytes) was included as an additional control. Exposure times vary between panels and do not accurately reflect relative abundances. (**G**) AID–GFP or AID–Flag/HA were immunoprecipitated in the presence of 1 mg/ml DNase and/or 0.5 mg/ml RNase using the corresponding anti-tag antibodies from lysates of HEK293T cell contransfected with Flag–DnaJa1 or Myc–DnaJa2, respectively, and analysed by western blot.

or Hsp90 had no effect on AID or Ig gene conversion in DT40 (Figure 3D–F).

We then asked whether depletion of DnaJa1 would have the predicted opposite effect to its overexpression. We transduced CH12F3 cells with different shRNAs targeting murine DnaJa1. Each of them decreased DnaJa1 protein to a different extent (from ∼70 to 30% of the control; Figure 4A and B), which was mirrored by a proportional decrease in isotype

switching to IgA (Figure 4C and D). Importantly, the relative reductions in CSR and in DnaJa1 were linearly correlated (Figure 4E). Depletion of DnaJa1 reduced AID protein levels (Figure 4F) but did not affect *Aicda* or Iα germline transcription, nor did it impact cell growth kinetics or Hsc70 or Hsp90 levels (Supplementary Figure S2). In contrast, efficient knockdown of DnaJa2 in CH12F3 cells had no effect on CSR or AID protein levels (Figure 4G–J). Finally, DnaJa2

Table I (Co)chaperones identified by mass spectrometry copurifying with tagged AID from Ramos B-cell extracts

HUGO name	Description	AID–Flag/HA pull-down[a]	AID–GFP pull-down		
			Peptide number	Mascot score	Coverage (%)
DNAJA1	Hsp40 homologue, subfamily A, member 1	×	47	1232	65
DNAJA2	Hsp40 homologue, subfamily A, member 2		39	1003	60
DNAJA3	Hsp40 homologue, subfamily A, member 3		9	207	14
HSPA8	Heat shock 70 kDa protein 8 isoform 1	×	19	517	19
HSP90AA1	Heat shock 90 kDa protein 1, α	×	39	1101	25
HSP90AB1	Heat shock 90 kDa protein 1, β	×	81	2010	48
AHSA1	AHA1, activator of heat shock 90 kDa protein ATPase homologue 1	×	19	480	28
BAG2	BCL2-associated athanogene 2 (Hsp70-cochaperone)		16	327	39
TCP1	T-complex polypeptide 1	×	5	154	6
CCT6A	T-complex protein 1 subunit ζ	×	1	84	3
CCT4	T-complex protein 1 subunit δ	×	3	60	7
CCT7	T-complex protein 1 subunit η		1	56	5

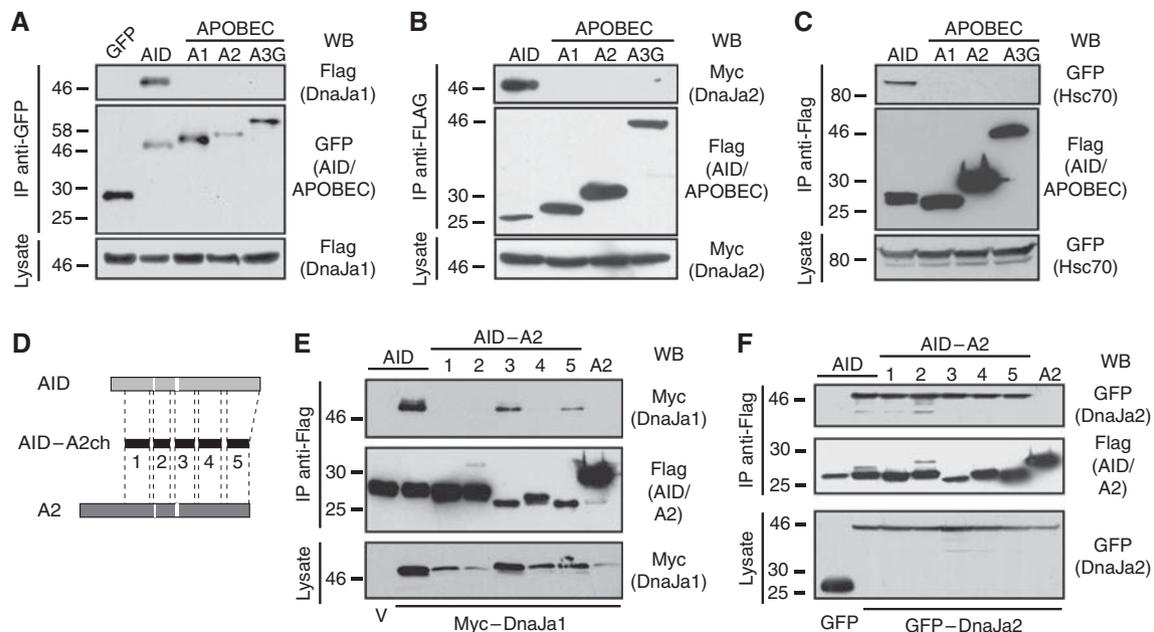[a]Data are from Orthwein et al (2010).

Figure 2 AID but not the APOBECs interacts with DnaJa1, DnaJa2 and Hsc70 in vitro. (**A**) GFP-tagged versions of AID, the indicated APOBECs or GFP control were transiently cotransfected with Flag–DnaJa1 into HEK293T cells and immunoprecipitated with anti-GFP. Immunoprecipitates were probed by western blot. (**B**) As in (**A**) but using Flag-tagged versions of AID and the APOBECs cotransfected with Myc–DnaJa2 and immunoprecipitated with anti-Flag. (**C**) As in (**B**) but cotransfected with GFP–Hsc70. One of the two independent experiments is shown for (**A–C**). (**D**) Schematic representation of AID–APOBEC2 chimeric proteins (AID–A2ch1–5) in which either one of the regions from A2 indicated between dotted lines was substituted into the homologous AID region. (**E**) Flag-tagged versions of AID, A2 or the AID-2 chimeras were immunoprecipitated using anti-Flag from HEK293T cell lysates cotransfected with Myc–DnaJa1 and analysed by western blot. (**F**) Flag-tagged versions of AID, A2 or the AID-2 chimeras were immunoprecipitated using anti-Flag from HEK293T cell lysates cotransfected with GFP–DnaJa2 and analysed by western blot.

depletion had no effect on AID half-life while DnaJa1 depletion reduced it by half (Figure 4K and L). Altogether these results suggest a non-redundant and limiting role for DnaJa1 in determining the levels of functional AID partaking in its stabilization.

Compromised antibody immune response in DnaJa1-deficient mice

The only phenotype observed so far in $DNAJA1^{-/-}$ mice is a defect in spermatogenesis likely due to abnormal androgen receptor signalling (Terada et al, 2005). Our findings

prompted the analysis of the antibody response in these mice. Flow cytometry analysis of lymphocyte populations showed little difference between $DNAJA1^{-/-}$ and control mice lymphocyte populations. The only statistically significant changes were a 10% decrease in the proportion of follicular B cells and an ~2-fold increase in marginal zone B cells in the spleen (Supplementary Figure S3). In contrast, there was a consistent 50% deficiency in isotype switching to IgG1 in splenic naive B cells from $DNAJA1^{-/-}$ mice stimulated ex vivo compared with their $DNAJA1^{+/+}$ or $DNAJA1^{+/-}$ controls (Figure 5A and B). The defect in CSR
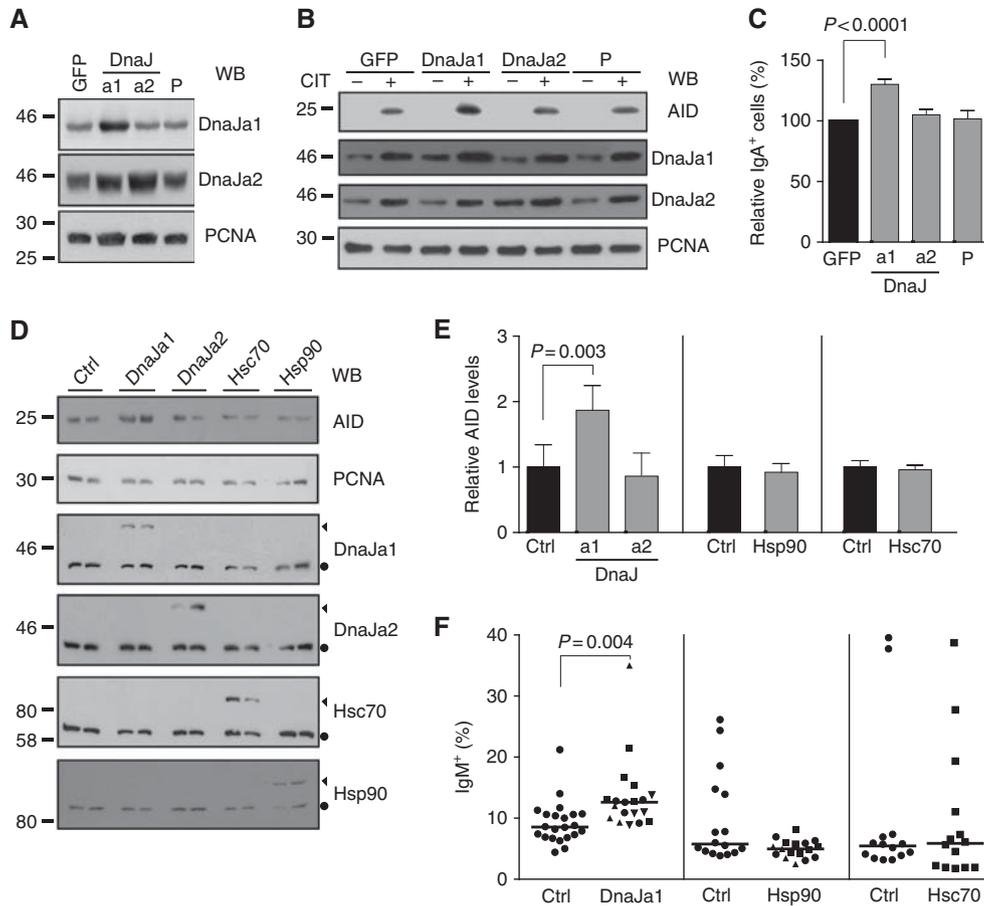
Figure 3 DnaJa1 overexpression increases AID levels and antibody gene diversification. (**A**) CH12F3 mouse B cells transduced with pMX–ires–GFP vector either empty (GFP) or encoding untagged DnaJa1 or DnaJa2 were sorted for GFP-expressing cells, lysed and analysed by western blot using anti-DnaJa1 or anti-DnaJa2 and anti-PCNA as loading control. P, parental cells. (**B**) Endogenous AID from transduced and parental CH12F3 cells was analysed by western blot using the indicated antibodies before (−) and 24 h after (+) stimulation with agonist anti-CD40, IL-4 and TGF-β1 (CIT). (**C**) Proportion of IgA$^+$ CH12F3 cells at day 3 post-CIT. The mean proportion of IgA$^+$ cells determined by flow cytometry ± s.d. from six independent stimulations is plotted for each population relative to the GFP controls set as 100%. (**D**) Endogenous AID was analysed by western blot using anti-AID on cell lysates from two representative, independently derived stable DT40 cell clones transfected with empty vector (Ctrl) or plasmids encoding myc–DnaJa1, myc–Dnaja2, myc–Hsp90 or GFP–Hsc70. Specific antibodies against each protein detected the transfected (triangles) and endogenous (circles) proteins. PCNA was used as loading control. (**E**) Endogenous AID levels quantified by densitometry from unsaturated western blots similar to those shown in (**D**) and normalized to the corresponding PCNA level. The mean value for AID in control samples set as 1 was used to normalize all values in each experiment. Data expressed as mean values ± s.d. of multiple subclones for each construct are plotted (myc–DnaJa1 $n = 15$ and myc–DnaJa2 $n = 21$ versus controls $n = 18$; myc–Hsp90β $n = 11$ versus controls $n = 11$; GFP–Hsc70 $n = 12$ versus controls $n = 12$). (**F**) Ig gene conversion frequency in transfected DT40 cells was estimated as the median proportion of IgM$^+$ cells arising from multiple IgM$^−$ subclones after 4 weeks of clonal expansion. The proportion of sIgM$^+$ for each subclone and median values are plotted. Different symbols indicate subclones obtained from independent transfectants. In all panels, P-values from unpaired, one-tailed t-test are indicated only for significant differences ($P < 0.05$).

was also clear when comparing cells that have undergone the same number of cell divisions without any sign of increased cell death in $DNAJA1^{−/−}$ cells (Figure 5C; Supplementary Figure S4). In fact, there were no differences in proliferation, $Aicda$, Iμ or Iγ1 germline transcription in $DNAJA1^{−/−}$ versus control activated B cells (Supplementary Figure S4). Western blots showed a consistent 50% decrease in AID protein levels in activated B cells from each $DNAJA1^{−/−}$ mouse compared with their littermate controls (Figure 5D). DnaJa1-deficient mice had similar IgM and IgG1 serum levels than controls (Figure 5E). This was expected since the long lifespan of plasma cells and antigen-mediated selection allow substantial accumulation of switched Ig isotypes in the serum of AID haploinsufficient or $MSH2^{−/−}$ mice, which have defects of similar magnitude in AID levels and/or CSR as those we observe (Rada et al, 2004; Sernández et al, 2008; Takizawa

et al, 2008). DnaJa1-deficient mice had impaired response to immunization with the T-cell-dependent antigen 4-hydroxy-3-nitrophenylacetyl-conjugated chicken γ globulin (NP-CGG). There was a significant decrease in the titre of total as well as high affinity anti-NP IgG1 during the primary response in all six $DNAJA1^{−/−}$ mice analysed (Figure 5F), demonstrating a CSR defect in vivo. By the secondary response anti-NP titres remained lower than controls in only half of them so only a non-significant trend was apparent when analysing the group (Figure 5F). Unlike androgen signalling defects and slightly reduced body weight, which are only found in $DNAJA1^{−/−}$ males (Terada et al, 2005), there was no sex bias for the phenotypes reported here.

We conclude that DnaJa1 deficiency causes a B-cell intrinsic defect in CSR, most likely by reducing AID protein levels, thus delaying antibody immune responses.
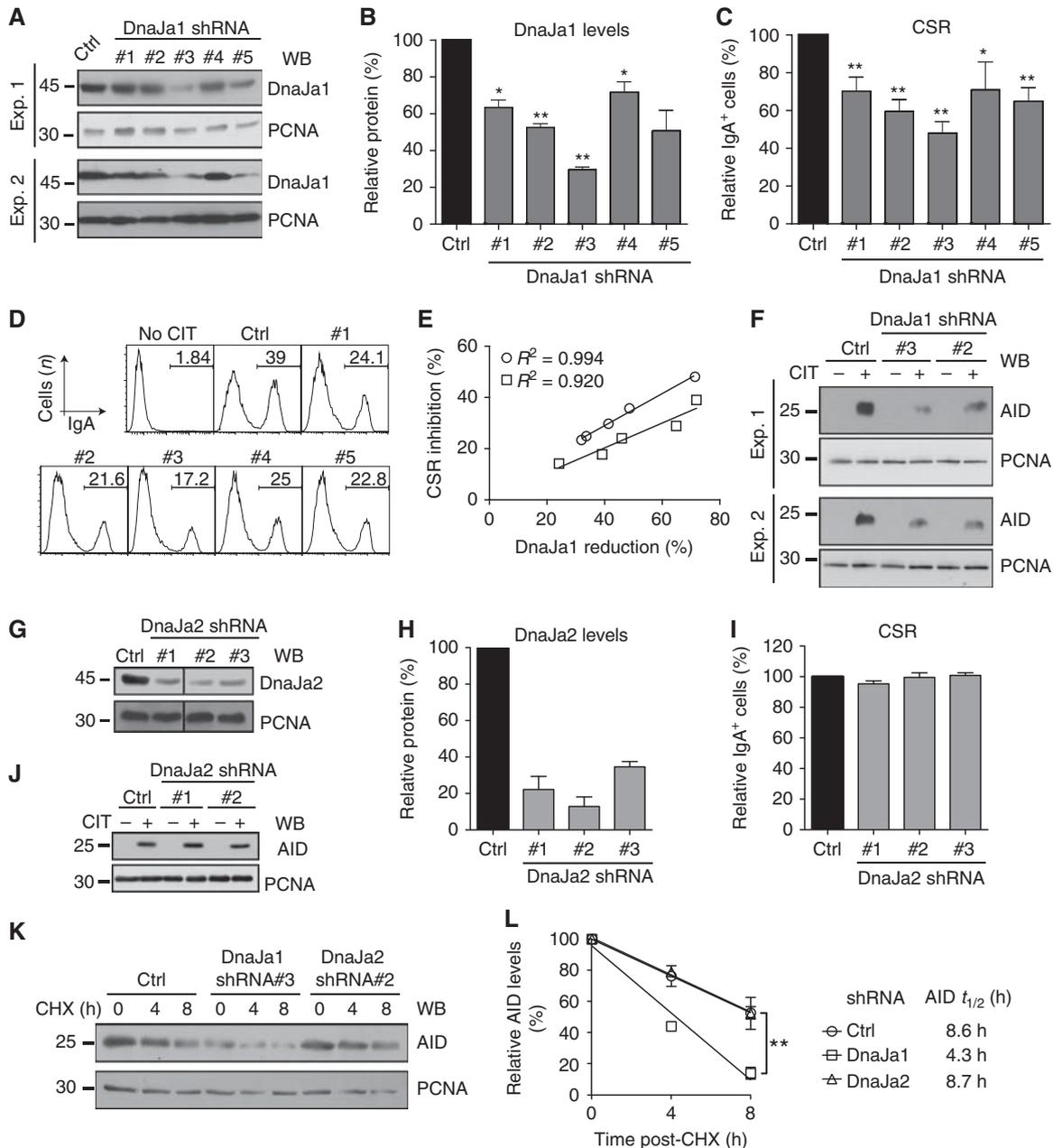
Figure 4 Reduced AID levels and CSR in DnaJa1-depleted CH12F3 cells. (**A**) CH12F3 cells were transduced with a lentiviral vector carrying control shRNA (Ctrl) or one of five different mouse DnaJa1-specific shRNAs (#1–#5), selected on puromycin and analysed by western blot for DnaJa1 and PCNA as loading control. Populations obtained from two independent infections are shown. (**B**) DnaJa1 protein levels were estimated by densitometry from western blots of three independently infected populations and normalized to each corresponding PCNA signal. Data expressed as mean values ± s.d. for each DnaJa1 shRNA are plotted relative to DnaJa1 levels in control shRNA cells set as 100% (*$P<0.01$, **$P<0.0005$, paired one-tailed t-test). (**C**) Proportion of IgA$^+$ cells at day 3 post-CIT as determined for flow cytometry for the same populations used for (**B**). Data expressed as mean values ± s.d. from six independent inductions are plotted relative to the IgA$^+$ proportion in control shRNA cells set as 100% (*$P<0.005$, **$P<0.0005$ in paired one-tailed t-test). (**D**) Representative flow cytometry profiles of transduced CH12F3 stimulated with CIT for 3 days or not (no CIT) and stained with anti-IgA. The proportion of IgA$^+$ cells is indicated in each histogram. (**E**) The mean reduction in CSR versus the mean reduction in DnaJa1 protein for each shRNA was plotted for two independent experiments (circles and squares) and analysed by linear regression. The correlation coefficients (R^2) are indicated. (**F**) Western blots from two independent experiments measuring AID in CH12F3 cells transduced with control or DnaJa1 shRNAs, 24 h post-CIT. (**G**) CH12F3 cells transduced with control shRNA (ctrl) or one of three different mouse DnaJa2-specific shRNAs (#1–#3) were analysed as in (**A**). One of the two independent experiments is shown. (**H**) DnaJa2 protein levels were estimated and plotted as in (**B**). (**I**) The proportion of IgA$^+$ cells at day 3 post-CIT in control versus DnaJa2-depleted cells was determined and plotted as in (**C**). (**J**) Western blot measuring AID in CH12F3 cells transduced with control or DnaJa2 shRNAs, 24 h post-CIT. (**K**) AID levels were measured by western blot 24 h post-CIT in CH12F3 cells transduced with shRNA control, DnaJa1 shRNA#3 or DnaJa2 shRNA#2 at 0, 4 and 8 h after treatment with 100 ng/ml CHX. PCNA is used as a loading control. One of the two independent experiments is shown. (**L**) AID protein levels after CHX treatment were estimated by densitometry from western blots of two independent experiments, normalized to each corresponding PCNA signal. Data expressed as mean values ± s.e.m. for each time point are plotted with AID levels at $t=0$ h set as 100%. AID protein half-lives were calculated and are indicated.
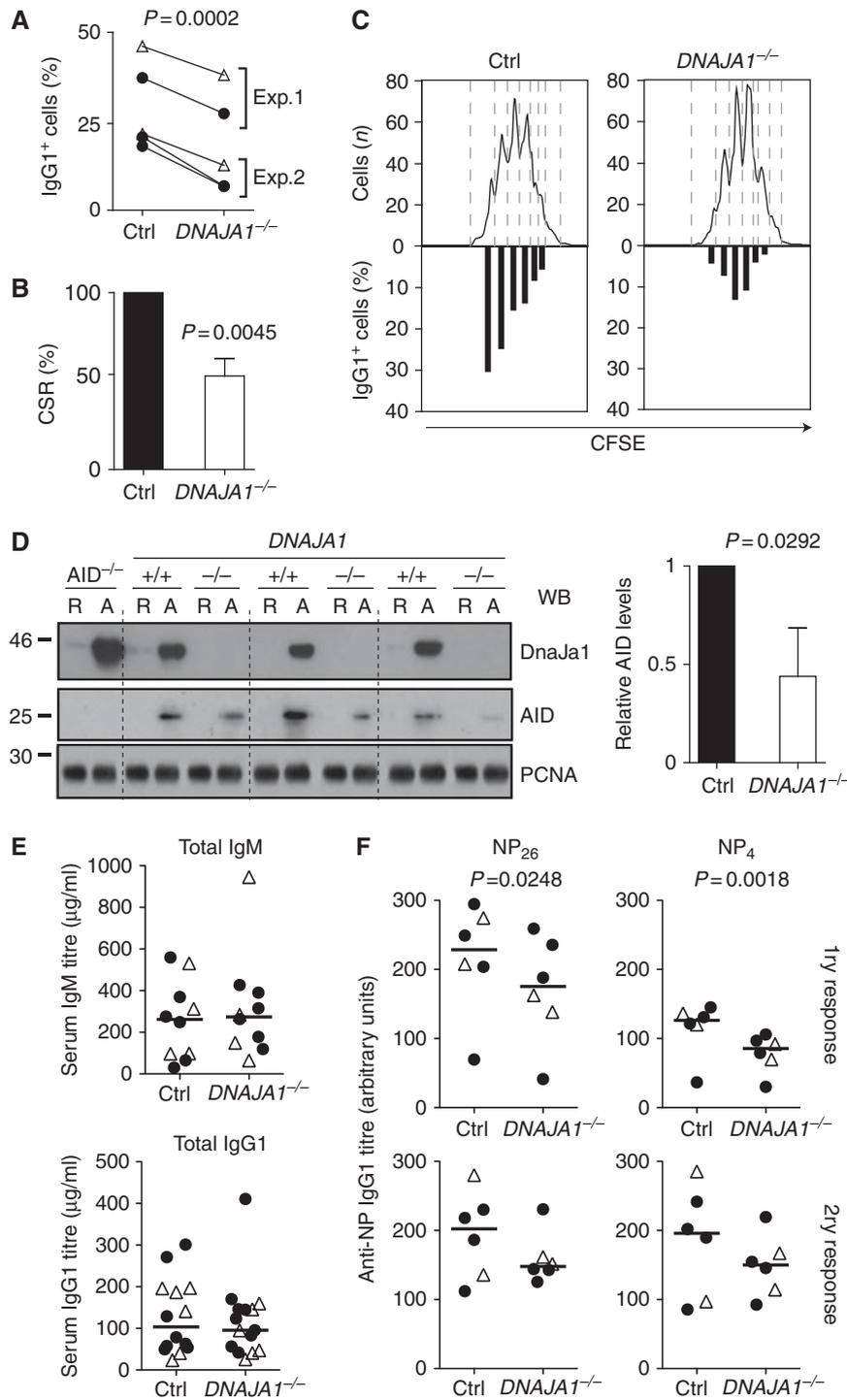
Figure 5 Reduced AID protein levels and isotype switching in $DNAJA1^{-/-}$ mice. (**A**) Proportion of IgG1$^+$ cells in purified splenic B cells from five $DNAJA1^{-/-}$ and control ($+/+$ or $+/-$) mice 4 days post-IL-4 and LPS stimulation, measured by flow cytometry. Two independent experiments are plotted in the same graph. A line links littermate pairs, with females (triangles) and males (circles) distinguished. (**B**) The data from (**A**) were compiled by normalizing the IgG1$^+$ B-cell proportion from each of the $DNAJA1^{-/-}$ mice to its paired control set as 100%. The mean relative CSR $\pm$ s.d. value for $DNAJA1^{-/-}$ mice is plotted. (**C**) Splenic naive B cells from $DNAJA1^{-/-}$ mice and littermate controls were loaded with CFSE, activated with IL-4 and LPS for 4 days and the proportion of IgG1$^+$ cells for each cell division determined by flow cytometry. One representative out of four mice pairs analysed is plotted. (**D**) DnaJa1, AID and PCNA protein levels were analysed by western blot in lysates from resting (R) or LPS + IL-4-activated (A) splenic B cells purified from three $DNAJA1^{-/-}$ and their matched control littermates (pairs separated by dashed lines). AID levels in each mouse were quantified by densitometry, normalized to PCNA levels and the mean $\pm$ s.d. AID levels for $DNAJA1^{-/-}$ mice relative to their corresponding littermate are plotted in the right-hand panel. (**E**) Concentration of IgM and IgG1 in sera from 3- to 5-month-old $DNAJA1^{-/-}$ or littermate control mice determined by ELISA. Each dot represents an individual mouse with females (triangles) and males (circles) distinguished. Horizontal lines indicate median values. (**F**) Six littermate pairs of control and $DNAJA1^{-/-}$ mice were immunized with NP$_{15}$-CGG and serum samples collected at day 11 post-immunization (primary response). The mice were boosted at day 30 and sera collected again at day 37 (secondary response). Anti-NP IgG1 titres were determined by ELISA using plates coated with NP$_{26}$-BSA (NP$_{26}$ column, total anti-NP antibodies) or NP$_4$-BSA (NP$_4$ column, high affinity anti-NP antibodies). The value for each mouse is indicated, distinguishing females (triangles) and males (circles) with lines indicating median values. In all panels, P-values from paired, one-tailed Student's t-test are indicated only for statistically significant differences ($P < 0.05$).

DnaJa1-mediated stabilization of AID depends on its farnesylation

Since we have shown that AID is an Hsp90 client (Orthwein et al, 2010) and Hsp40s partake in the Hsp90 molecular chaperoning pathway (Kimura et al, 1995; Young et al, 2004), we sought some evidence linking DnaJa1 to Hsp90, in addition to the decrease in AID stability observed after Dnaja1 depletion (see Figure 4L). Molecular details about the link between Hsp40 and Hsp90 in vivo are scarce but it has been shown that Ydj1 farnesylation is necessary for maintaining the protein levels of Hsp90 clients in yeast (Flom et al, 2008). We first determined which domains of DnaJa1 mediated interaction with AID. CoIP of AID with DnaJa1 truncated variants showed that the CTDI, a Ydj1 substrate-binding site (Li et al, 2003), as well as the Zn-fingers domain were dispensable for the interaction. Indeed, deletion of the N-terminal 160 amino acids of DnaJa1 destroys the structure of both these domains (Figure 6A and B) but still allowed AID interaction (Figure 6C). Mutating the farnesyl group acceptor Cys (Caplan et al, 1992) abolished the interaction of DnaJa1 with AID (Figure 6D). Thus, the CTDIII and farnesylation are the minimal requirements for DnaJa1 binding to AID. More importantly, while DnaJa1 expression was able to complement the CSR defect in $DNAJA1^{-/-}$ B cells, expression of the DnaJa1-C394S was not able to; nor was DnaJa2 further suggesting a specific role for DnaJa1 (Figure 6E–G). To confirm that the AID levels were dependent on farnesylated DnaJa1, we treated the Ramos human B-cell line and mouse primary B cells with the farnesyltransferase inhibitor FTI-277. Increasing doses of FTI-277 correlated with the accumulation of non-farnesylated DnaJa1 and a concomitant decrease in AID protein levels in both cases (Figure 6H) without affecting Aicda transcription (Supplementary Figure S5). Furthermore, FTI treatment was able to decrease ex-vivo isotype switching to IgG1 in mouse B cells (Figure 6I–K). Confocal microscopy of cotransfected cells showed that AID shuttled independently of DnaJa1 localization, which was not obviously affected by the C394S mutation (Figure 6L). In fact, DnaJa1 depletion in CH12F3 cells had no effect on AID localization or shuttling (Supplementary Figure S5).

Taken together, these results indicate that AID biological activity levels depend on farnesylated DnaJa1 through a mechanism that determines AID protein levels in the cytoplasm.

Discussion

We have previously identified AID as an Hsp90 client, with this interaction being critical for AID stability (Orthwein et al, 2010). We now show the interaction of AID with the Hsp40–Hsc70 system and with DnaJa1 in particular. The remarkable specificity of the functional interaction between AID and DnaJa1 in vitro and in vivo provides insight not only on AID biology but also into the functional specialization of Hsp40s.

The Hsp40–Hsp70 system delivers a subset of its substrates to the Hsp90 molecular chaperoning pathway for their functional stabilization (Young et al, 2004; Hartl et al, 2011). Indeed, AID folding and stabilization shows similarities with the stabilization cycle of steroid hormone receptors (Picard, 2006; Hartl et al, 2011) and our results suggest the identity and function of many of the molecules involved (Orthwein et al, 2010 and this work). DnaJa1 could act as cochaperone of Hsc70 by stimulating its ATPase activity to initiate a folding cycle that is completed by Hsp70 nucleotide exchange factors (Young et al, 2004; Kampinga and Craig, 2010; Terada and Oike, 2010). We speculate BAG2 could be the Hsc70 nucleotide exchange factor in this cycle since it was the only one that copurified with AID (Table I). Hsp40–Hsp70 and Hsp90 are coupled by Sti1, which has been copurified with AID (Okazaki et al, 2011) and may link the ternary AID–Hsp40–Hsp70 complex to Hsp90.

Although DnaJa1 may well be an Hsc70 cochaperone during AID folding, the fact that different Hsp40s can at least partially substitute for each other in this role (Johnson and Craig, 2001; Cintron and Toft, 2006), combined with the non-redundant function that DnaJa1 has in determining AID cellular levels in vivo, suggest that DnaJa1 may have another, more specific function. There is considerable genetic and biochemical evidence showing that Hsp40 is a functional component of some of the complexes during the Hsp90

Figure 6 DnaJa1 farnesylation is necessary to maintain AID levels and for CSR. (**A**) DnaJa1 domains illustration indicating the deletions and single point mutation variants used. CaaX indicates the farnesylation motif where Cys394 was mutated to Ser in DnaJa1ΔF. (**B**) Crystal structure of the yeast DnaJa1 orthologue Ydj1 substrate-binding domain using the same colour scheme as in (**A**). Residues homologous to those truncated in DnaJa1ΔN2, which destroy CTDI and II, are in grey. A Ydj1 substrate peptide, which cocrystalized bound to CTDI, is shown as filled model. Data are from pdb1NLT (Li et al, 2003). (**C**) Flag-tagged AID or A2 were immunoprecipitated using anti-Flag from lysates of HEK293T cells cotransfected with the indicated GFP-tagged DnaJa1 variants and analysed by WB. One of the two independent experiments is shown. (**D**) Similar experiment to (**C**) but using Myc-tagged DnaJa1 variants. One of the two independent experiments is shown. (**E**) Splenic B cells purified from $DNAJA1^{+/+}$ and $DNAJA1^{-/-}$ mice activated with LPS and IL-4, transduced with retroviruses expressing control (GFP), DnaJa1–, DnaJa1ΔF– or DnaJa2-ires–GFP and analysed at day 4 post-infection by flow cytometry. Histograms show GPF-gated cells stained with anti-IgG1 indicating the proportion of IgG1$^+$ cells for one representative out of three mice analysed. (**F**) Compilation of ex-vivo CSR data from three $DNAJA1^{-/-}$ mice complemented as in (**E**). The proportion of IgG1$^+$ cells for the $DNAJA1^{-/-}$ B cells expressing each transduced protein is shown relative to the value obtained for the corresponding $DNAJA1^{+/+}$ littermate B cells infected with control GFP vector, set as 100%. Paired, two-tailed t-test was used to evaluate significance ($P<0.05$). (**G**) Transduced splenic B cells were analysed by western blot with anti-DnaJa1 and anti-DnaJa2 using anti-GFP as loading control. (**H**) Ramos B-lymphoma cells and purified mouse splenic B cells were treated with the indicated concentrations of the farnesyltransferase inhibitor FTI-277 for 72 h and the levels of AID and farnesylated (circle) and non-farnesylated (triangle) DnaJa1 analysed by western blot. PCNA was used as loading control. (**I**) Experimental strategy used for assaying CSR in mouse splenic B cells after farnesyltransferase inhibition. D, day. (**J**) Relative proportion of IgG1$^+$ cells measured by flow cytometry in mouse splenic B cells treated with the farnesyl transferase inhibitor FTI-277 or solvent control as in (**I**). (**K**) CFSE staining profile of the cells used for (**I**) with the proportion of IgG1$^+$ cells for each cell division plotted below. (**L**) Hela cells cotransfected with GFP-tagged DnaJa1 or DnaJa1ΔF and untagged AID were treated with leptomycin B or heat shocked for 90 min at 43°C, fixed, stained with anti-AID and anti-mouse Alexa-680 and imaged by confocal microscopy. Representative confocal images are shown, scale bar = 10 μm. The cellular localization of each protein was classified and the proportion of cotransfected cells showing each distribution is plotted as bars with the number of cells counted indicated (n). C, cytoplasmic; N, nuclear.

cycle (Caplan *et al*, 1995; Kimura *et al*, 1995; Dittmar *et al*, 1998; Kosano *et al*, 1998; Hernández *et al*, 2002; Wegele *et al*, 2006; Flom *et al*, 2008). Three observations suggest that DnaJa1 has a specific role in AID stabilization and link this activity to Hsp90. First, AID is less stable in cells depleted of DnaJa1. Second, DnaJa1 farnesylation is required for binding to and optimal CSR activity of AID just as Ydj1 farnesylation

is required for its interaction with Hsp90 clients (Flom *et al*, 2008). Cytoplasmic type I Hsp40s are isoprenylated (Caplan *et al*, 1992; Kanazawa *et al*, 1997). Although farnesylation targets a minor proportion of Ydj1 to intracellular membranes (Caplan *et al*, 1992), this seems to be in no small part by contributing to protein–protein interactions (Marshall, 1993). Indeed, the farnesylated CTDIII domain of DnaJa1 mediates
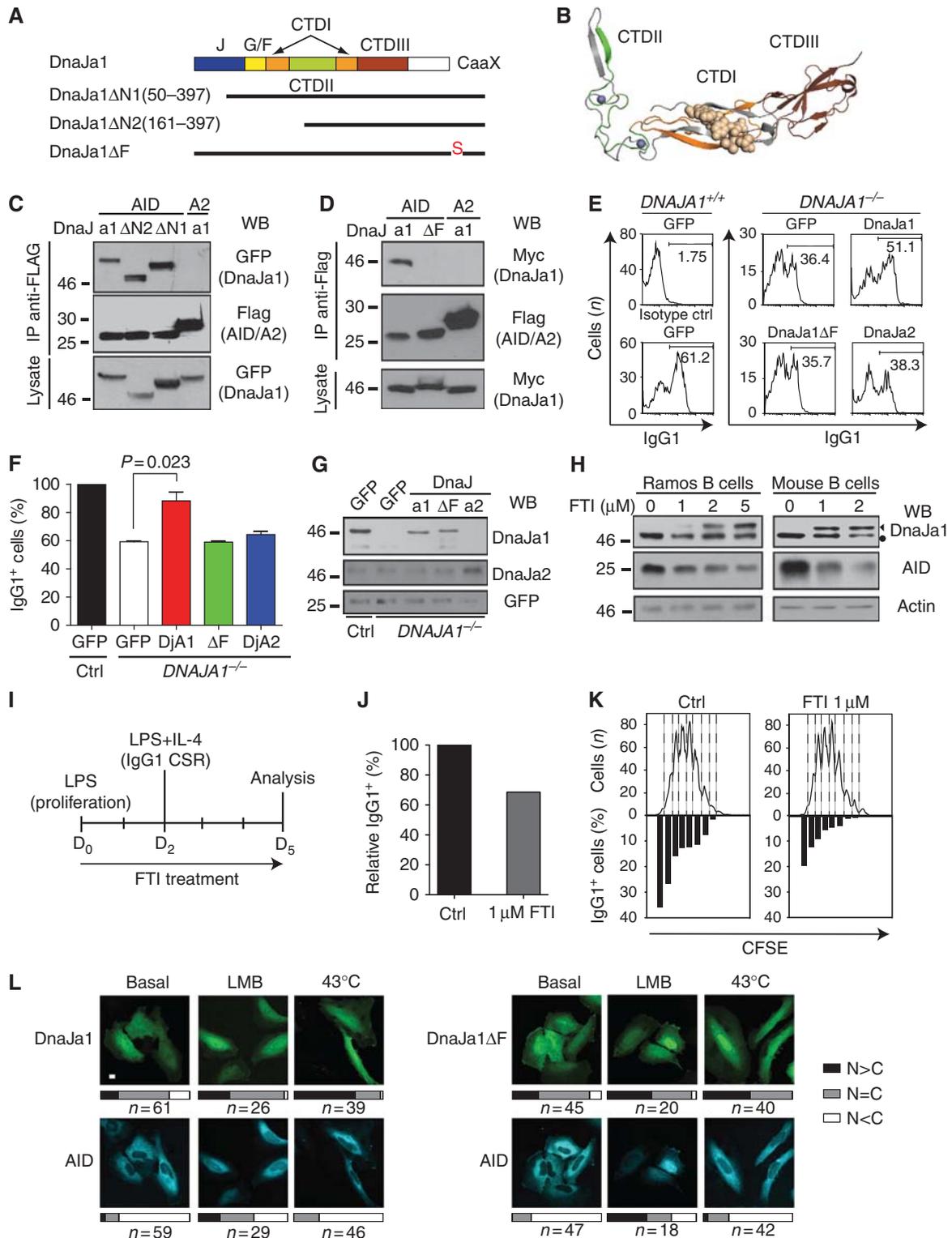
AID binding instead of the CTDI, a characterized Ydj1 substrate-binding domain (Li et al, 2003). Coincidently, the Ydj1 mutant found to compromise Hsp90 clients stability in yeast had a single point mutation in CTDIII (Kimura et al, 1995). Third, $DNAJA1^{-/-}$ mice can only make 50% of the normal AID protein levels, indicating that no other J-protein is fully redundant with DnaJa1. DnaJa2 would be the obvious back-up in $DNAJA1^{-/-}$ cells since it is very similar to DnaJa1, well expressed in B cells and interacts with AID in vitro. However, this is not the case since AID and CSR are reduced proportionally to DnaJa1 depletion in CH12F3 cells (despite abundant DnaJa2 expression) while DnaJa2 depletion or overexpression do not change AID levels, nor can DnaJa2 rescue CSR in $DNAJA1^{-/-}$ B cells. An analogous specificity was observed for the potassium channel HERG with depletion of DnaJa1, but not DnaJa2, reducing the intracellular trafficking of HERG (Walker et al, 2010). Interestingly, like AID, HERG stability depends on Hsp90 (Ficker et al, 2003). It is interesting that most AID–APOBEC2 chimeras disrupt DnaJa1 binding while they all bind to DnaJa2. One could speculate that DnaJa1 recognizes a certain structure, which would be easily altered in the chimeras, while DnaJa2 may recognize less specific hydrophobic motifs present in earlier folding intermediates. Our results are compatible with some specialization of DnaJa1 to work in the Hsp90 pathway but defining this will require further work. The experiments with HERG were done in transfected HeLa cells and there is in fact hardly any data about protein levels of endogenous Hsp90 clients in the absence of a particular DjA in any system. In yeast, the Ste11 kinase levels are reduced by Ydj1 deficiency (Flom et al, 2008). In $DNAJA1^{-/-}$ mice, the androgen and glucocorticoid receptors were increased (Terada et al, 2005) while AID is reduced. This nicely illustrates the existence of different subpathways for folding/stabilization of Hsp90 clients. To the best of our knowledge, AID is the first Hsp90 client identified in higher eukaryotes that requires a specific Hsp40 to maintain its physiological levels in vivo.

If DnaJa2 is not able to complement DnaJa1 deficiency and DnaJa4, the only other cytoplasmic DjA, is not expressed, it is interesting to speculate how the residual AID is folded and stabilized in vivo in $DNAJA1^{-/-}$ lymphocytes. Whichever pathway forms AID in $DNAJA1^{-/-}$ B cells, it is clearly not fully redundant with DnaJa1. At least in yeast, the DjB Sis1 can partially substitute for Ydj1 (Lu and Cyr, 1998; Johnson and Craig, 2001). Thus, a DjB like DnaJb1 or even DnaJa2 could substitute for DnaJa1 in early Hsp70-assisted AID folding; and/or it could proceed via the CCT chaperonin (Young et al, 2004; Hartl et al, 2011). The end result is anyhow much less efficient. Therefore, we hypothesize that a later DnaJa1 role must exist in vivo, probably by linking AID to the Hsp90 pathway, and/or helping in assembling some AID complexes. This role would be more specific than, and thereby limiting, compared with protein biogenesis.

The fact that the response of $DNAJA1^{-/-}$ mice to immunization is so similar to the one observed in AID haploinsufficient mice (Sernández et al, 2008; Takizawa et al, 2008) suggests that the defect in CSR in vivo reflects the 50% reduction in AID rather than any other unknown defect on immune cell function. Beyond any small differences, the phenotypes of $Aicda^{+/-}$ and $DNAJA1^{-/-}$ mice indicate that AID can be limiting for antibody diversification and that

reduced AID levels, no matter their cause, are detrimental for antibody responses, which could be exploited for therapy. We have shown that Hsp90 inhibitors could be used in this way (Orthwein et al, 2010). DnaJa1 now offers alternative possibilities by linking AID protein levels to protein farnesylation. Farnesyltransferase inhibitors have promising anti-cancer activity but their relevant targets are incompletely understood (Sebti and Der, 2003). We show that it is indeed possible to reduce AID levels and function by using farnesyltransferase inhibitors, which could have therapeutic value to modulate AID.

Hsp40s are limiting components in chaperone networks. In E. coli, DnaJ is present in a 1:10 ratio with respect to DnaK (Hsp70) (Bardwell et al, 1986). In yeast, the relative molecular proportion of Hsp82 (Hsp90), Ssa1 (Hsp70) and Ydj1 can be estimated at $\sim 4{:}2{:}1$, respectively (Ghaemmaghami et al, 2003). Hsp40s can also be functionally limiting in mammalian systems (Minami et al, 1996; Dittmar et al, 1998; Heldens et al, 2010). We indeed see a modest increase in AID levels upon DnaJa1 overexpression. We would not expect a dramatic increase since DnaJa1 surely has many substrates and is distributed among all of them and so would be any excess DnaJa1. Considering that we achieve ~ 2-fold increase in DnaJa1 levels, the fact that we can see an increase in AID levels and activity is significant and suggest that DnaJa1 is indeed limiting for AID folding and/or stabilization. This raises the question of whether DnaJa1 overexpression in certain cases, such as EBV infection (Young et al, 2008) or its association with antibody-mediated autoimmune diseases (Ramos et al, 2011) could contribute to disease by increasing AID levels.

Materials and methods

Cell lines and drug treatments
The Ramos Burkitt's B-cell lymphoma lines stably expressing GFP, AID–GFP or AID–Flag/HA have been described (Patenaude et al, 2009; Orthwein et al, 2010). Chicken DT40 B-lymphoma cells stably expressing myc–DnaJa1, myc–DnaJa2 or myc–Hsp90β were obtained by electroporation as described (Sale et al, 2001). GFP–Hsc70 was introduced by retroviral infection. CH12F3 mouse B cells stably expressing DnaJa1, DnaJa2, AID–GFP or empty vectors were generated by retroviral delivery of pMXs-ires–GFP or pMXs constructs and sorted for GFP-expressing cells. FTI-277 (Sigma-Aldrich) was diluted in water at 1 mM and stored at $-20°C$. Cycloheximide (CHX) (Sigma-Aldrich) was freshly prepared before each experiment and diluted in EtOH at 100 μg/ml.

Identification of AID partners
The yeast two-hybrid screening has been described (Conticello et al, 2008). Ramos B cells stably expressing AID–GFP were lysed on ice in 50 mM Tris–HCl pH 8, 150 mM NaCl, 1% Triton X-100, 5 mM $MgCl_2$, 100 μg/ml RNase, 100 μg/ml DNase and complete protease inhibitors cocktail (Roche) at 3×10^8 cells/ml. AID was immunoprecipitated using anti-GFP-coated magnetic microbeads and MACS separation columns (Miltenyi Biotec) following the manufacturer's instructions. Eluted proteins were separated by SDS–PAGE and silver stained. Differential bands compared with the pattern obtained from Ramos cells expressing GFP only were excised and submitted to mass spectrometry for protein identification as described (Orthwein et al, 2010).

DNA constructs
AID–GFP, AID–Flag/HA, APOBECs and Myc–Hsp90β expression vectors have been described (Orthwein et al, 2010). Human DnaJa1 in pFlag–CMV2 was a kind gift of Dr HY Zoghbi (Baylor College of Medicine, Houston). Human Hsc70 in pEGFP-C1 was a kind gift from Dr U Stochaj (McGill University, Montreal). Human DnaJa2,

DnaJa4, DnaJb1 and DnaJb11 were obtained from the I.M.A.G.E consortium. Details on DNA constructs are provided in Supplementary data.

Retroviral and lentiviral infections

Retroviral transduction of mouse primary B cells and DT40 cells was as described (Patenaude et al, 2009). CH12F3 B cells were infected with retroviral particles obtained from the supernatant of HEK293T cell cultures cotransfected with pMXs-ires–GFP or pMXs constructs and vectors expressing MLV Gag-Pol and VSV-G envelope (2:1:1 ratio). Briefly, the retroviral supernatant was spun down at $2000\,g$ for 90 min at $32\,°C$ in Retronectin® (Takara)-coated plates before adding 5×10^5 CH12F3 cells and spinning at $600\,g$ for 30 min at $32\,°C$ and GFP + cells were sorted. A similar procedure was used for lentiviral infections. Mission® DnaJa1 and DnaJa2 shRNAs (Supplementary Table SII) cloned in pLKO.1-Puro (Sigma-Aldrich) were contransfected with psPAX2 (Addgene plasmid 12260, deposited by Dr D Trono) and pVSG-G into HEK293T cells to produce lentiviral particles. An shRNA targeting luciferase and cloned in pLKO.1-Puro (Addgene plasmid 1864 deposited by Dr D Sabatini) was used as control. Cells were selected in $0.5\,µg/ml$ puromycin 2 days post-infection.

IP and western blot

Cells were homogenized in lysis buffer (20 mM Tris, pH 8.0, 137 mM NaCl, 10% glycerol, 2 mM EDTA, 1% Triton X-100, 20 mM NaF) 48 h after transfection and extracted on ice for 10 min. The lysate was clarified for 10 min at $12\,000\,g$ at $4\,°C$ and processed for western blot or IP. Typically, $2–5 \times 10^6$ cells were analysed by western blots to detect endogenous proteins. Tagged proteins were immunoprecipitated using either anti-Flag M2 affinity gel (Sigma-Aldrich) or MACS GFP Isolation kit (Miltenyi Biotech) according to the manufacturer's instructions. Eluates and lysates were analysed by western blot developed with SuperSignal West Pico Chemiluminescent substrate (Thermo Fisher Scientific). Antibodies used are in Supplementary data.

Monitoring of antibody diversification

Ig gene conversion was estimated by fluctuation assay of the proportion of cells undergoing surface IgM− to IgM+ reversion in multiple single cell-derived populations of DT40 cells after 3-week expansion at $41\,°C$. IgM expression was measured by flow cytometry using 1:200 PE- (Southern Biotech) or FITC (Bethyl)-conjugated anti-chicken IgM. IgM to IgA switching was assayed in CH12F3-2 cells activated for 3 days with 1 ng/ml TGF-β1, 10 ng/ml IL-4 and 1 µg/ml agonist anti-CD40 (BD). IgA expression was measured by flow cytometry using anti-mouse IgA-PE antibody (1:200; eBioscience). Ex-vivo isotype switching to IgG1 was assayed using resting splenic B cells purified by CD43 depletion, with CFSE loading to monitor cell division where indicated, as described (Orthwein et al, 2010). Cells were stained with anti-IgG1-biotin (1:200; BD) followed by APC-conjugated anti-biotin (Miltenyi Biotech) and 10 µg/ml propidium iodide. For the complementation assays of $DNAJA1^{-/-}$ B cells using retroviral delivery, double infection was performed at days 2 and 3 post-stimulation and isotype switching analysed at day 5.

Mice immunizations and lymphocyte populations

$DNAJA1^{-/-}$ mice (Terada et al, 2005) were backbred to C57Bl/6J background for at least 11 generations. In all experiments, 2- to 4-month-old, sex-matched littermates were used. $DNAJA1^{+/+}$ and $DNAJA1^{+/-}$ served as controls as they were indistinguishable (our results and Terada et al, 2005). Mice were immunized i.p. with 100 µg of NP_{15}-CGG (Biosearch Technologies Inc., # N5055-5) in 100 µl PBS + 100 µl of Imject Alum (Thermo Scientific) and boosted at day 30. Blood samples were collected at day −1 (preimmune), day 11 post-immunization (primary response) and day 37 (secondary response). Anti-isotype-specific antibodies were used to capture and detect total serum IgM and IgG1 in serum by ELISA. Concentrations were estimated from calibration curves made with Ig isotype standards (BD Pharmingen). Serum levels of total or high affinity anti-NP-specific IgG1 were determined by coating plates with NP_{26}-BSA or NP_4-BSA (5 µg/well), respectively. IgG1 was detected using biotynilated anti-mouse IgG1 (1:1000; BD Pharmingen) followed by HRP-conjugated streptavidin (1:5000; Thermo Scientific) and 2,2′-Azino-bis(3-ethylbenzothiazoline-6-sulfonic acid) substrate, detected by absorbance at 405 nm. Arbitrary units were calculated multiplying OD readings for each point of a curve made of serial twofold dilutions of the serum by the corresponding serum dilution factor. The OD 50% was defined as the anti-NP IgG1 titre for each mouse and plotted divided by 100 (NP_{26}) or 10 (NP_4) to have similar graphing scales. Lymphocyte populations from spleen and thymus were analysed by flow cytometry as detailed in Supplementary data. The IRCM's and Kumamoto University's animal experimentation ethics committees approved all mouse work.

IF and confocal microscopy

HeLa cells were transiently cotransfected with AID in pCDNA3.1 and either pEGFP-C3 DnaJa1 or DnaJa1-C394S using TransIT-LT1 (Mirus). Cells were treated 48 h post-transfection either by heat shocking at $43\,°C$ for 90 min, or with 50 ng/ml Leptomycin B or EtOH solvent control for 2 h. Cells were processed for IF and confocal microscopy as described (Patenaude et al, 2009), except that blocking was 5% goat serum 1 mg/ml BSA in PBS overnight at $4\,°C$ and we used a mouse anti-AID MAb (clone, 1:500; Invitrogen) for 1 h followed by goat anti-mouse Alexa-680 (1:500; Invitrogen) for 30 min and imaged in an LSM 510 microscope (Zeiss) with a HeNe 633 laser. Control and DnaJa1-depleted CH12F3 cells stably expressing AID–GFP or GFP and DnaJa1 were treated with 10 ng/ml Leptomycin B or EtOH for 2 h. Cells were plated on poly-L-Lysine-treated coverslips and processed for confocal microscopy.

Supplementary data

Supplementary data are available at The EMBO Journal Online (http://www.embojournal.org).

Conflict of interest

The authors declare that they have no conflict of interest.

References

Aoufouchi S, Faili A, Zober C, D'Orlando O, Weller S, Weill J-C, Reynaud C-A (2008) Proteasomal degradation restricts the nuclear lifespan of AID. J Exp Med 205: 1357–1368

Arakawa H, Hauschild J, Buerstedde J-M (2002) Requirement of the activation-induced deaminase (AID) gene for immunoglobulin gene conversion. Science 295: 1301–1306

Bardwell JC, Tilly K, Craig E, King J, Zylicz M, Georgopoulos C (1986) The nucleotide sequence of the Escherichia coli K12 dnaJ + gene. A gene that encodes a heat shock protein. J Biol Chem 261: 1782–1785

Bhangoo MK, Tzankov S, Fan ACY, Dejgaard K, Thomas DY, Young JC (2007) Multiple 40-kDa heat-shock protein chaperones

function in Tom70-dependent mitochondrial import. *Mol Biol Cell* **18:** 3414–3428

Brar SS, Watson M, Diaz M (2004) Activation-induced cytosine deaminase (AID) is actively exported out of the nucleus but retained by the induction of DNA breaks. *J Biol Chem* **279:** 26395–26401

Caplan AJ, Langley E, Wilson EM, Vidal J (1995) Hormone-dependent transactivation by the human androgen receptor is regulated by a dnaJ protein. *J Biol Chem* **270:** 5251–5257

Caplan AJ, Tsai J, Casey PJ, Douglas MG (1992) Farnesylation of YDJ1p is required for function at elevated growth temperatures in Saccharomyces cerevisiae. *J Biol Chem* **267:** 18890–18895

Cintron NS, Toft DO (2006) Defining the requirements for Hsp40 and Hsp70 in the Hsp90 chaperone pathway. *J Biol Chem* **281:** 26235–26244

Conticello SG, Ganesh K, Xue K, Lu M, Rada C, Neuberger MS (2008) Interaction between antibody-diversification enzyme AID and spliceosome-associated factor CTNNBL1. *Mol Cell* **31:** 474–484

Di Noia JM, Neuberger MS (2007) Molecular mechanisms of antibody somatic hypermutation. *Annu Rev Biochem* **76:** 1–22

Dittmar KD, Banach M, Galigniana MD, Pratt WB (1998) The role of DnaJ-like proteins in glucocorticoid receptor.hsp90 heterocomplex assembly by the reconstituted hsp90.p60.hsp70 foldosome complex. *J Biol Chem* **273:** 7358–7366

Ficker E, Dennis AT, Wang L, Brown AM (2003) Role of the cytosolic chaperones Hsp70 and Hsp90 in maturation of the cardiac potassium channel HERG. *Circ Res* **92:** e87–e100

Flom GA, Lemieszek M, Fortunato EA, Johnson JL (2008) Farnesylation of Ydj1 is required for *in vivo* interaction with Hsp90 client proteins. *Mol Biol Cell* **19:** 5249–5258

Ghaemmaghami S, Huh WK, Bower K, Howson RW, Belle A, Dephoure N, O'Shea EK, Weissman JS (2003) Global analysis of protein expression in yeast. *Nature* **425:** 737–741

Gur E, Katz C, Ron EZ (2005) All three J-domain proteins of the Escherichia coli DnaK chaperone machinery are DNA binding proteins. *FEBS Lett* **579:** 1935–1939

Hartl FU, Bracher A, Hayer-Hartl M (2011) Molecular chaperones in protein folding and proteostasis. *Nature* **475:** 324–332

Heldens L, Dirks RP, Hensen SMM, Onnekink C, van Genesen ST, Rustenburg F, Lubsen NH (2010) Co-chaperones are limiting in a depleted chaperone network. *Cell Mol Life Sci* **67:** 4035–4048

Hernández MP, Chadli A, Toft DO (2002) HSP40 binding is the first step in the HSP90 chaperoning pathway for the progesterone receptor. *J Biol Chem* **277:** 11873–11881

Ito S, Nagaoka H, Shinkura R, Begum NA, Muramatsu M, Nakata M, Honjo T (2004) Activation-induced cytidine deaminase shuttles between nucleus and cytoplasm like apolipoprotein B mRNA editing catalytic polypeptide 1. *Proc Natl Acad Sci USA* **101:** 1975–1980

Johnson JL, Craig EA (2001) An essential role for the substrate-binding region of Hsp40s in Saccharomyces cerevisiae. *J Cell Biol* **152:** 851–856

Kampinga HH, Craig EA (2010) The HSP70 chaperone machinery: J proteins as drivers of functional specificity. *Nat Rev Mol Cell Biol* **11:** 579–592

Kanazawa M, Terada K, Kato S, Mori M (1997) HSDJ, a human homolog of DnaJ, is farnesylated and is involved in protein import into mitochondria. *J Biochem* **121:** 890–895

Kimura Y, Yahara I, Lindquist S (1995) Role of the protein chaperone YDJ1 in establishing Hsp90-mediated signal transduction pathways. *Science* **268:** 1362–1365

Kosano H, Stensgard B, Charlesworth MC, McMahon N, Toft D (1998) The assembly of progesterone receptor-hsp90 complexes using purified proteins. *J Biol Chem* **273:** 32973–32979

Kuraoka M, Holl TM, Liao D, Womble M, Cain DW, Reynolds AE, Kelsoe G (2011) Activation-induced cytidine deaminase mediates central tolerance in B cells. *Proc Natl Acad Sci USA* **108:** 11560–11565

Langer T, Lu C, Echols H, Flanagan J, Hayer MK, Hartl FU (1992) Successive action of DnaK, DnaJ and GroEL along the pathway of chaperone-mediated protein folding. *Nature* **356:** 683–689

Li J, Qian X, Sha B (2003) The crystal structure of the yeast Hsp40 Ydj1 complexed with its peptide substrate. *Structure* **11:** 1475–1483

Liu M, Duke JL, Richter DJ, Vinuesa CG, Goodnow CC, Kleinstein SH, Schatz DG (2008) Two levels of protection for the

B cell genome during somatic hypermutation. *Nature* **451:** 841–845

Lu Z, Cyr DM (1998) Protein folding activity of Hsp70 is modified differentially by the hsp40 co-chaperones Sis1 and Ydj1. *J Biol Chem* **273:** 27824–27830

Macduff D, Demorest Z, Harris R (2009) AID can restrict L1 retro-transposition suggesting a dual role in innate and adaptive immunity. *Nucleic Acids Res* **37:** 1854–1867

Marshall CJ (1993) Protein prenylation: a mediator of protein-protein interactions. *Science* **259:** 1865–1866

Matsumoto Y, Marusawa H, Kinoshita K, Endo Y, Kou T, Morisawa T, Azuma T, Okazaki IM, Honjo T, Chiba T (2007) Helicobacter pylori infection triggers aberrant expression of activation-induced cytidine deaminase in gastric epithelium. *Nat Med* **13:** 470–476

McBride KM, Barreto V, Ramiro AR, Stavropoulos P, Nussenzweig MC (2004) Somatic hypermutation is limited by CRM1-dependent nuclear export of activation-induced deaminase. *J Exp Med* **199:** 1235–1244

Minami Y, Höhfeld J, Ohtsuka K, Hartl FU (1996) Regulation of the heat-shock protein 70 reaction cycle by the mammalian DnaJ homolog, Hsp40. *J Biol Chem* **271:** 19617–19624

Morgan HD, Dean W, Coker HA, Reik W, Petersen-Mahrt SK (2004) Activation-induced cytidine deaminase deaminates 5-methylcytosine in DNA and is expressed in pluripotent tissues: implications for epigenetic reprogramming. *J Biol Chem* **279:** 52353–52360

Muramatsu M, Kinoshita K, Fagarasan S, Yamada S, Shinkai Y, Honjo T (2000) Class switch recombination and hypermutation require activation-induced cytidine deaminase (AID), a potential RNA editing enzyme. *Cell* **102:** 553–563

Muramatsu M, Sankaranand VS, Anant S, Sugai M, Kinoshita K, Davidson NO, Honjo T (1999) Specific expression of activation-induced cytidine deaminase (AID), a novel member of the RNA-editing deaminase family in germinal center B cells. *J Biol Chem* **274:** 18470–18476

Nakamura M, Kondo S, Sugai M, Nazarea M, Imamura S, Honjo T (1996) High frequency class switching of an IgM+ B lymphoma clone CH12F3 to IgA+ cells. *Int Immunol* **8:** 193–201

Okazaki IM, Hiai H, Kakazu N, Yamada S, Muramatsu M, Kinoshita K, Honjo T (2003) Constitutive expression of AID leads to tumorigenesis. *J Exp Med* **197:** 1173–1181

Okazaki IM, Okawa K, Kobayashi M, Yoshikawa K, Kawamoto S, Nagaoka H, Shinkura R, Kitawaki Y, Taniguchi H, Natsume T, Iemura S-I, Honjo T (2011) Histone chaperone Spt6 is required for class switch recombination but not somatic hypermutation. *Proc Natl Acad Sci USA* **108:** 7920–7925

Orthwein A, Patenaude A-M, Affar EB, Lamarre A, Young JC, Di Noia JM (2010) Regulation of activation-induced deaminase stability and antibody gene diversification by Hsp90. *J Exp Med* **207:** 2751–2765

Pasqualucci L, Bhagat G, Jankovic M, Compagno M, Smith P, Muramatsu M, Honjo T, Morse III HC, Nussenzweig MC, Dalla-Favera R (2008) AID is required for germinal center-derived lymphomagenesis. *Nat Genet* **40:** 108–112

Pasqualucci L, Guglielmino R, Houldsworth J, Mohr J, Aoufouchi S, Polakiewicz R, Chaganti RS, Dalla-Favera R (2004) Expression of the AID protein in normal and neoplastic B cells. *Blood* **104:** 3318–3325

Pasqualucci L, Neumeister P, Goossens T, Nanjangud G, Chaganti RS, Kuppers R, Dalla-Favera R (2001) Hypermutation of multiple proto-oncogenes in B-cell diffuse large-cell lymphomas. *Nature* **412:** 341–346

Patenaude AM, Di Noia JM (2010) The mechanisms regulating the subcellular localization of AID. *Nucleus* **1:** 325–331

Patenaude AM, Orthwein A, Hu Y, Campo VA, Kavli B, Buschiazzo A, Di Noia JM (2009) Active nuclear import and cytoplasmic retention of activation-induced deaminase. *Nat Struct Mol Biol* **16:** 517–527

Pauklin S, Sernández I, Bachmann G, Ramiro AR, Petersen-Mahrt SK (2009) Estrogen directly activates AID transcription and function. *J Exp Med* **206:** 99–111

Peled JU, Kuang FL, Iglesias-Ussel MD, Roa S, Kalis SL, Goodman MF, Scharff MD (2008) The biochemistry of somatic hypermutation. *Annu Rev Immunol* **26:** 481–511

Picard D (2006) Chaperoning steroid hormone action. *Trends Endocrinol Metab* **17:** 229–235

Qiu X-B, Shao Y-M, Miao S, Wang L (2006) The diversity of the DnaJ/Hsp40 family, the crucial partners for Hsp70 chaperones. *Cell Mol Life Sci* **63:** 2560–2570

Rada C, Di Noia JM, Neuberger MS (2004) Mismatch recognition and uracil excision provide complementary paths to both Ig switching and the A/T-focused phase of somatic mutation. *Mol Cell* **16:** 163–171

Ramiro AR, Jankovic M, Eisenreich T, Difilippantonio S, Chen-Kiang S, Muramatsu M, Honjo T, Nussenzweig A, Nussenzweig MC (2004) AID is required for c-myc/IgH chromosome translocations *in vivo*. *Cell* **118:** 431–438

Ramos PS, Williams AH, Ziegler JT, Comeau ME, Guy RT, Lessard CJ, Li H, Edberg JC, Zidovetzki R, Criswell LA, Gaffney PM, Graham DC, Graham RR, Kelly JA, Kaufman KM, Brown EE, Alarcón GS, Petri MA, Reveille JD, Mcgwin G *et al* (2011) Genetic analyses of interferon pathway-related genes reveal multiple new loci associated with systemic lupus erythematosus. *Arthritis Rheum* **63:** 2049–2057

Revy P, Muto T, Levy Y, Geissmann F, Plebani A, Sanal O, Catalan N, Forveille M, Dufourcq-Labelouse R, Gennery A, Tezcan I, Ersoy F, Kayserili H, Ugazio AG, Brousse N, Muramatsu M, Notarangelo LD, Kinoshita K, Honjo T, Fischer A *et al* (2000) Activation-induced cytidine deaminase (AID) deficiency causes the autosomal recessive form of the Hyper-IgM syndrome (HIGM2). *Cell* **102:** 565–575

Robbiani DF, Bothmer A, Callen E, Reina-San-Martin B, Dorsett Y, Difilippantonio S, Bolland DJ, Chen HT, Corcoran AE, Nussenzweig A, Nussenzweig MC (2008) AID is required for the chromosomal breaks in c-myc that lead to c-myc/IgH translocations. *Cell* **135:** 1028–1038

Robbiani DF, Bunting S, Feldhahn N, Bothmer A, Camps J, Deroubaix S, McBride KM, Klein IA, Stone G, Eisenreich TR, Ried T, Nussenzweig A, Nussenzweig MC (2009) AID produces DNA double-strand breaks in non-Ig genes and mature B cell lymphomas with reciprocal chromosome translocations. *Mol Cell* **36:** 631–641

Sale JE, Calandrini DM, Takata M, Takeda S, Neuberger MS (2001) Ablation of XRCC2/3 transforms immunoglobulin V gene conversion into somatic hypermutation. *Nature* **412:** 921–926

Sebti SM, Der CJ (2003) Opinion: searching for the elusive targets of farnesyltransferase inhibitors. *Nat Rev Cancer* **3:** 945–951

Sernández IV, De Yébenes VG, Dorsett Y, Ramiro AR (2008) Haploinsufficiency of activation-induced deaminase for antibody diversification and chromosome translocations both *in vitro* and *in vivo*. *PLoS ONE* **3:** e3927

Sha B, Lee S, Cyr DM (2000) The crystal structure of the peptide-binding fragment from the yeast Hsp40 protein Sis1. *Structure* **8:** 799–807

Stavnezer J (2011) Complex regulation and function of activation-induced cytidine deaminase. *Trends Immunol* **32:** 194–201

Stavnezer J, Guikema JEJ, Schrader CE (2008) Mechanism and regulation of class switch recombination. *Annu Rev Immunol* **26:** 261–292

Storck S, Aoufouchi S, Weill J-C, Reynaud C-A (2011) AID and partners: for better and (not) for worse. *Curr Opin Immunol* **23:** 337–344

Takizawa M, Tolarová H, Li Z, Dubois W, Lim S, Callen E, Franco S, Mosaico M, Feigenbaum L, Alt FW, Nussenzweig A, Potter M, Casellas R (2008) AID expression levels determine the extent of cMyc oncogenic translocations and the incidence of B cell tumor development. *J Exp Med* **205:** 1949–1957

Teng G, Hakimpour P, Landgraf P, Rice A, Tuschl T, Casellas R, Papavasiliou FN (2008) MicroRNA-155 is a negative regulator of activation-induced cytidine deaminase. *Immunity* **28:** 621–629

Terada K, Mori M (2000) Human DnaJ homologs dj2 and dj3, and bag-1 are positive cochaperones of hsc70. *J Biol Chem* **275:** 24728–24734

Terada K, Oike Y (2010) Multiple molecules of Hsc70 and a dimer of DjA1 independently bind to an unfolded protein. *J Biol Chem* **285:** 16789–16797

Terada K, Yomogida K, Imai T, Kiyonari H, Takeda N, Kadomatsu T, Yano M, Aizawa S, Mori M (2005) A type I DnaJ homolog, DjA1, regulates androgen receptor signaling and spermatogenesis. *EMBO J* **24:** 611–622

Tzankov S, Wong MJH, Shi K, Nassif C, Young JC (2008) Functional divergence between co-chaperones of Hsc70. *J Biol Chem* **283:** 27100–27109

Uchiyama Y, Takeda N, Mori M, Terada K (2006) Heat shock protein 40/DjB1 is required for thermotolerance in early phase. *J Biochem* **140:** 805–812

Walker VE, Wong MJ, Atanasiu R, Hantouche C, Young JC, Shrier A (2010) Hsp40 chaperones promote degradation of the HERG potassium channel. *J Biol Chem* **285:** 3319–3329

Walsh P, saæ D, Law YC, Cyr DM, Lithgow T (2004) The J-protein family: modulating protein assembly, disassembly and translocation. *EMBO Rep* **5:** 567–571

Wegele H, Wandinger SK, Schmid AB, Reinstein J, Buchner J (2006) Substrate transfer from the chaperone Hsp70 to Hsp90. *J Mol Biol* **356:** 802–811

Wu Y, Li J, Jin Z, Fu Z, Sha B (2005) The crystal structure of the C-terminal fragment of yeast Hsp40 Ydj1 reveals novel dimerization motif for Hsp40. *J Mol Biol* **346:** 1005–1011

Yamane A, Resch W, Kuo N, Kuchen S, Li Z, Sun H-W, Robbiani DF, McBride K, Nussenzweig MC, Casellas R (2011) Deep-sequencing identification of the genomic targets of the cytidine deaminase AID and its cofactor RPA in B lymphocytes. *Nat Immunol* **12:** 62–69

Young JC, Agashe VR, Siegers K, Hartl FU (2004) Pathways of chaperone-mediated protein folding in the cytosol. *Nat Rev Mol Cell Biol* **5:** 781–791

Young P, Anderton E, Paschos K, White R, Allday MJ (2008) Epstein-Barr virus nuclear antigen (EBNA) 3A induces the expression of and interacts with a subset of chaperones and co-chaperones. *J Gen Virol* **89:** 866–877

Zaheen A, Martin A (2011) Activation-induced cytidine deaminase and aberrant germinal center selection in the development of humoral autoimmunities. *Am J Pathol* **178:** 462–471